Stem Cell Reports, Volume *11*

Supplemental Information

Status of KRAS in iPSCs Impacts upon Self-Renewal and Differentiation Propensity

Kenji Kubara, Kazuto Yamazaki, Yasuharu Ishihara, Takuya Naruto, Huan-Ting Lin, Ken Nishimura, Manami Ohtaka, Mahito Nakanishi, Masashi Ito, Kappei Tsukahara, Tomohiro Morio, Masatoshi Takagi, and Makoto Otsu

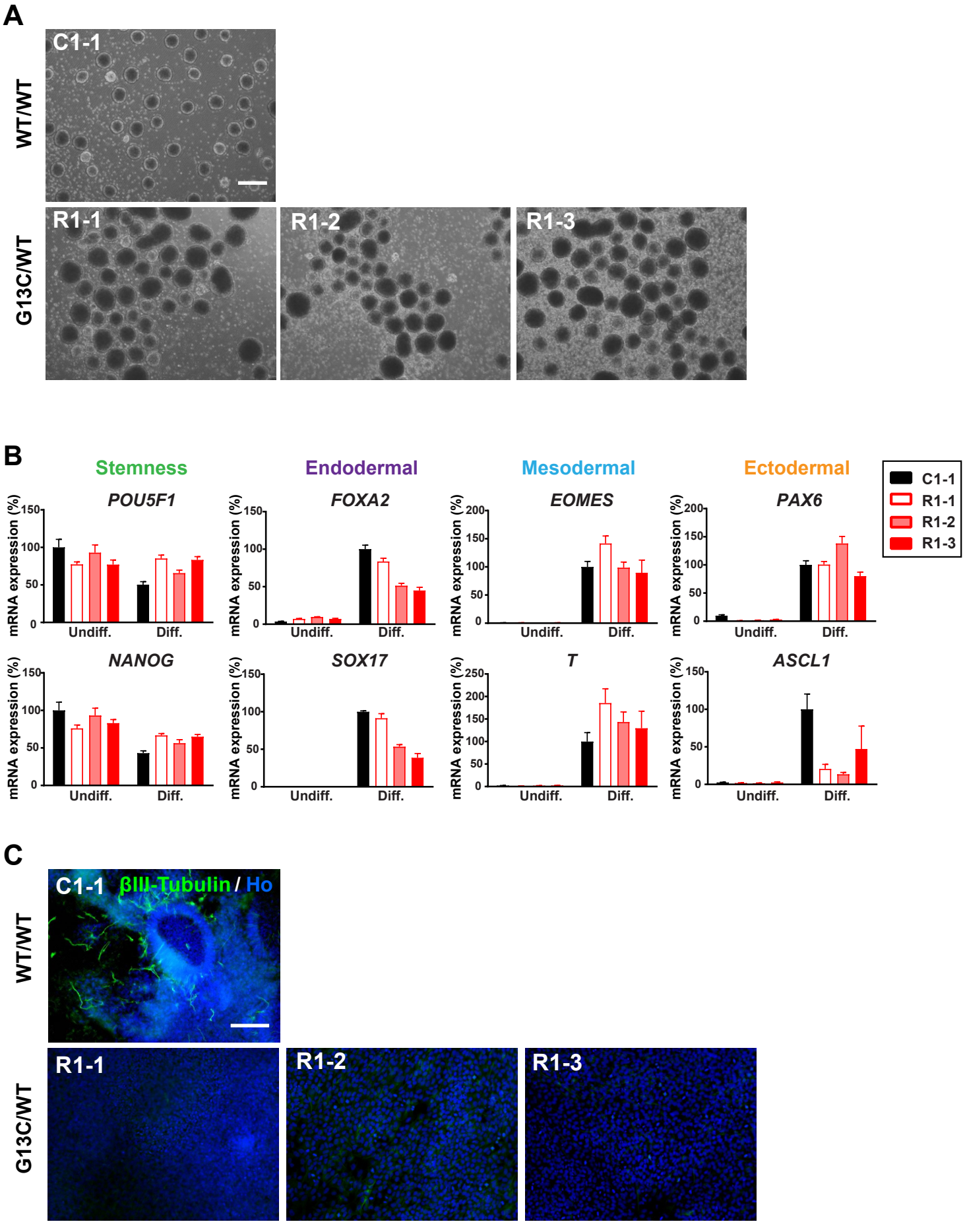
A
WT/WT
C1-1
G13C/WT
R1-1
R1-2
R1-3
B
Stemness
Endodermal
Mesodermal
Ectodermal
C1-1
R1-1
R1-2
R1-3
POU5F1
FOXA2
EOMES
PAX6
NANOG
SOX17
T
ASCL1
mRNA expression (%)
Undiff.
Diff.
C
WT/WT
C1-1 βIII-Tubulin / Ho
G13C/WT
R1-1
R1-2
R1-3

Figure S1. Different differentiation propensity between WT/WT and G13C/WT iPSCs from a case no. 1 RALD patient (Related to Figure 2)

(A) Embryoid body formation of case no. 1 iPSCs. Bar, 200 μm. (B) qRT-PCR analysis of 16-day differentiated cells from case no. 1 iPSCs. The following markers were used: *POU5F1* and *NANOG* for stemness; *FOXA2* and *SOX17* for endodermal; *T* and *EOMES* for mesodermal; and *ASCL1* and *PAX6* for ectodermal differentiation (n = 3 independent experiments; mean ± S.E.M.). Undiff. and Diff. mean undifferentiated iPSCs and differentiated cells. (C) Immnunocytochemistry of βIII-Tubulin in 16-day differentiated cells from case no. 1 iPSCs. Bar, 100 μm.

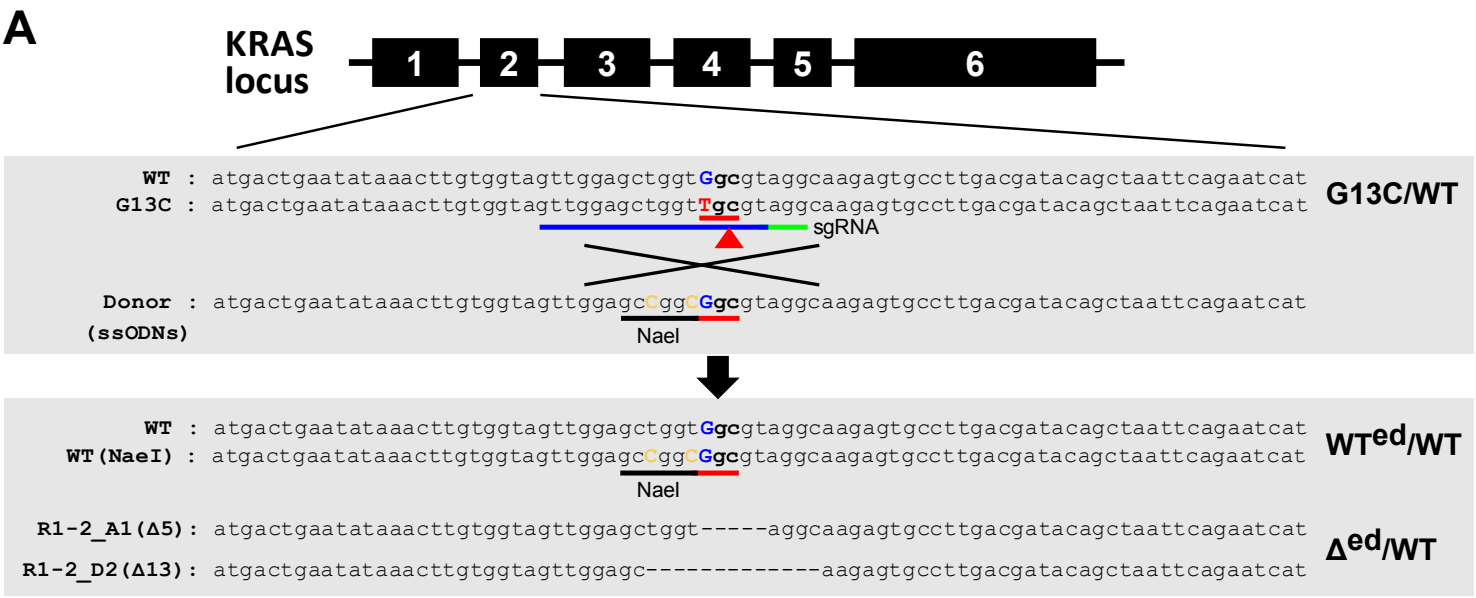

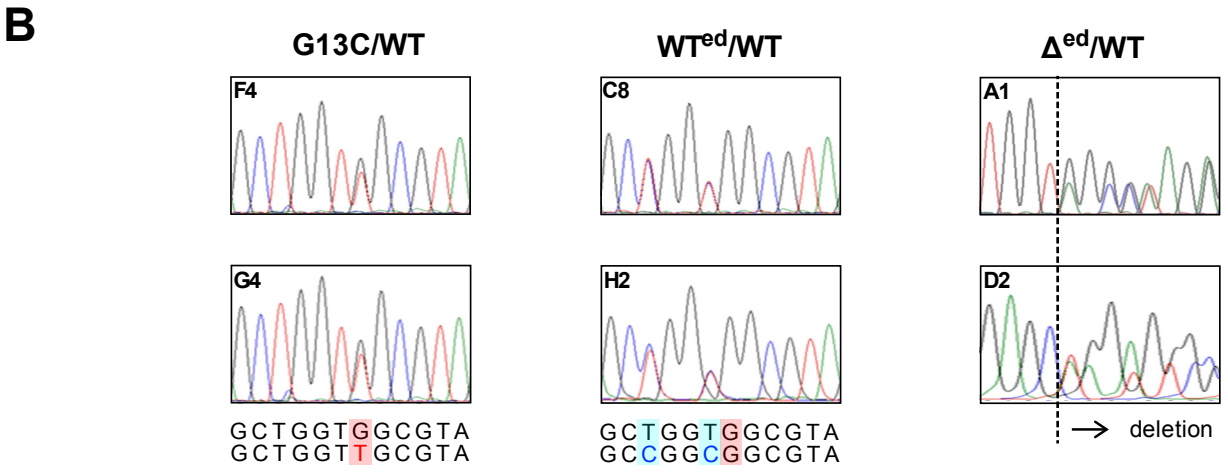

C

Target	Locus	Sequence (17 bp + PAM)	Mismatch	Gene
On (G13C)	chr12:25398274	GTTGGAGCTGGTTGCGTAGG	0	KRAS
On (WT)	chr12:25398274	GTTGGAGCTGGTGGCGTAGG	1	KRAS
Off-1	chr6:54635401	GTTGGAGCTGGTGGCGTAAG	1	None
Off-2	chr7:581706	GGTGAAGCTGGTTGCGTGGG	2	None
Off-3	chr7:581806	GGTGAAGCTGGTTGCGTGGG	2	None
Off-4	chr6:41204115	GCTGGAGCTGTTTGCGTAAG	2	None
Off-5	chr3:131104931	TCTGGAGATGGTTGCGTGGG	3	NUDT16

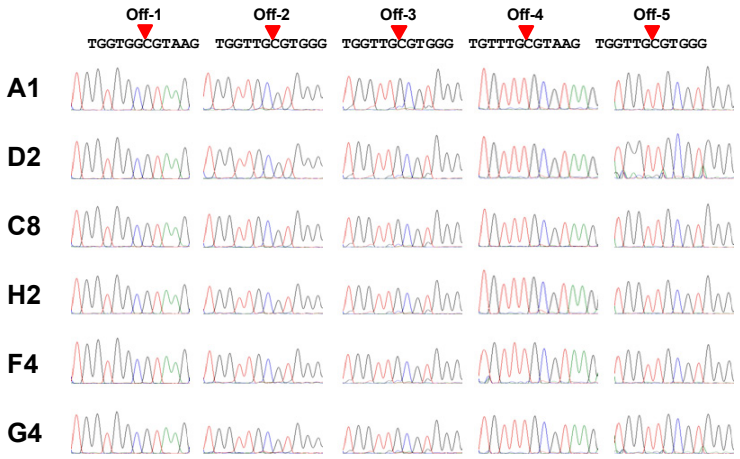

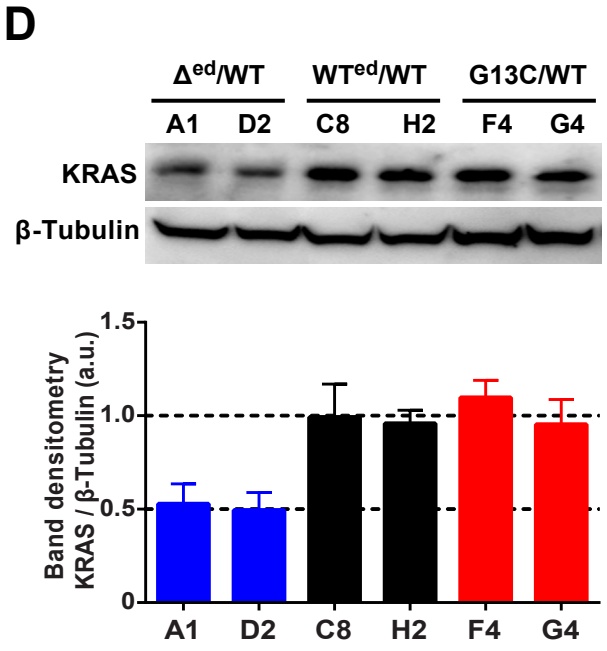

Figure S2. Rescue of KRAS mutation by using CRISPR/Cas9 (Related to Figures 2, 4, S3, and S4)

(A) A schematic overview of genome editing for *KRAS* using CRISPR/Cas9 system. G13C/WT iPSC clone (R1-2) derived from a case no. 1 RALD patient was used in this study. Red lines indicate the mutation and rescued site at G13 in *KRAS*. A single guide RNA (sgRNA) recognition site is shown by a blue line, and a protospacer adjacent motif (PAM) site is shown by a green line. A Cas9 cleavage site is shown by a red triangle. Silent mutations in *Nae*I site are shown by yellow letters. (B) Sequence analysis of genome-edited iPSC clones. (C) Sequence analysis against 5 off-target candidate sites in genome-edited iPSC clones. Mismatch sites are shown by red letters. The Cas9-cleavage sites are shown by red triangles. (D) Western blotting and densitometric analysis of KRAS and control β-Tubulin in genome-edited iPSC clones (n = 3 independent experiments; mean ± S.E.M.).

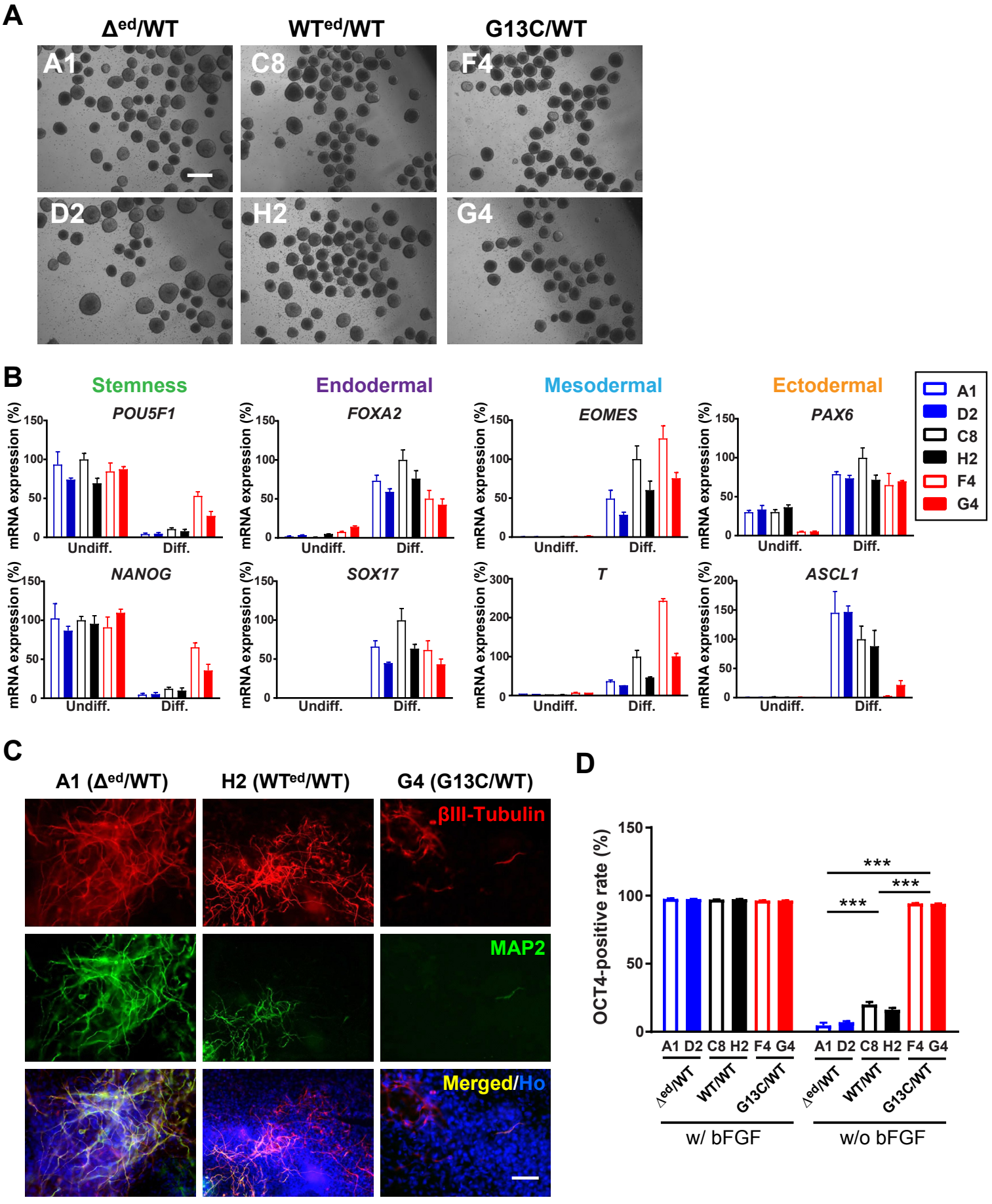
A
Δed/WT
WTed/WT
G13C/WT
A1
C8
F4
D2
H2
G4
B
Stemness
Endodermal
Mesodermal
Ectodermal
POU5F1
FOXA2
EOMES
PAX6
NANOG
SOX17
T
ASCL1
mRNA expression (%)
Undiff.
Diff.
A1
D2
C8
H2
F4
G4
C
A1 (Δed/WT)
H2 (WTed/WT)
G4 (G13C/WT)
βIII-Tubulin
MAP2
Merged/Ho
D
OCT4-positive rate (%)
***
***
***
A1 D2 C8 H2 F4 G4
Δed/WT
WT/WT
G13C/WT
w/ bFGF
w/o bFGF

Figure S3. Different differentiation propensity of genome-edited iPSC clones (Related to Figure 2 and 4)

(A) Embryoid body formation of genome-edited iPSC clones derived *KRAS* heterozygous mutant (G13C/WT) iPSC clone (R1-2). Heterozygous knockout (Δ^{ed}/WT; clones A1 and D2), rescued wild-type homozygous (WT^{ed}/WT; clones C8 and H2), and non-edited clones in spite of CRISPR/Cas9 treatment (G13C/WT; clones F4 and G4). Bar, 200 μm. (B) qRT-PCR analysis of 16-day differentiated cells from the genome-edited iPSC clones. The following markers were used: *POU5F1* and *NANOG* for stemness; *FOXA2* and *SOX17* for endodermal; *T* and *EOMES* for mesodermal; and *ASCL1* and *PAX6* for ectodermal differentiation (n = 3 independent experiments; mean ± S.E.M.). Undiff. and Diff. mean undifferentiated iPSCs and differentiated cells. (C) Immnunocytochemistry of βIII-Tubulin and MAP2 in 16-day differentiated cells from heterozygous knockout Δ^{ed}/WT (clone A1), rescued WT^{ed}/WT (clone H2), and not-edited G13C/WT iPSCs (clone G4). Bar, 50 μm. (D) Quantitative imaging analysis for OCT4 in genome-edited iPSC clones (n = 8 independent experiments; mean ± S.E.M.; *** $p < 0.001$; two-way ANOVA followed by Bonferroni's multiple comparison test).

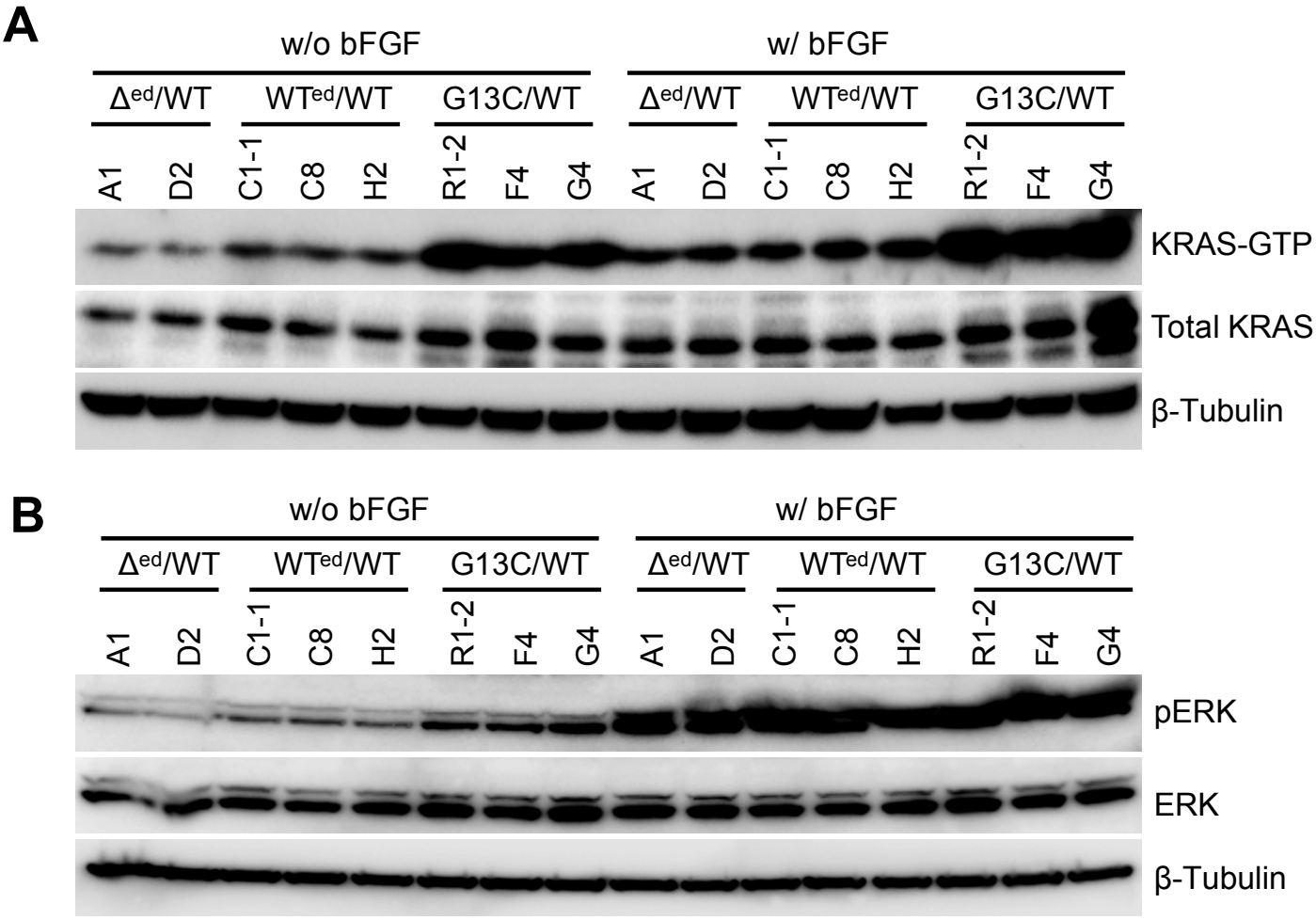
A
w/o bFGF
w/ bFGF
Δed/WT
WTed/WT
G13C/WT
A1
D2
C1-1
C8
H2
R1-2
F4
G4
KRAS-GTP
Total KRAS
β-Tubulin
B
pERK
ERK
β-Tubulin
C
Densitometry
KRAS-GTP / β-Tubulin (a.u.)
D
Densitometry
pERK / ERK (a.u.)

Figure S4. Biochemical analysis on the ERK and AKT pathways activity in genome-edited iPSC clones (Related to Figure 5)

(A) GST-RAF1 pull-down assays of genome-edited iPSC (Δ^{ed}/WT, WT^{ed}/WT, and G13C/WT) clones cultured with (w/) or without (w/o) bFGF for 3 days. β-Tubulin was used as an internal control. (B) Western blot analysis of genome-edited iPSC clones cultured w/ or w/o bFGF for 2 days. ERK and AKT were analyzed for their phosphorylation. (C) Densitometric analysis of western blotting results shown in (A) (n = 3 independent experiments; mean ± S.E.M.; $^{\#}$ $p = 0.0872$; *** $p < 0.001$; one-way ANOVA followed by Bonferroni's multiple comparison test). (D) Densitometric analysis of ERK in (B) (n = 3 independent experiments; mean ± S.E.M.; * $p < 0.05$; *** $p < 0.001$; one-way ANOVA followed by Bonferroni's multiple comparison test).

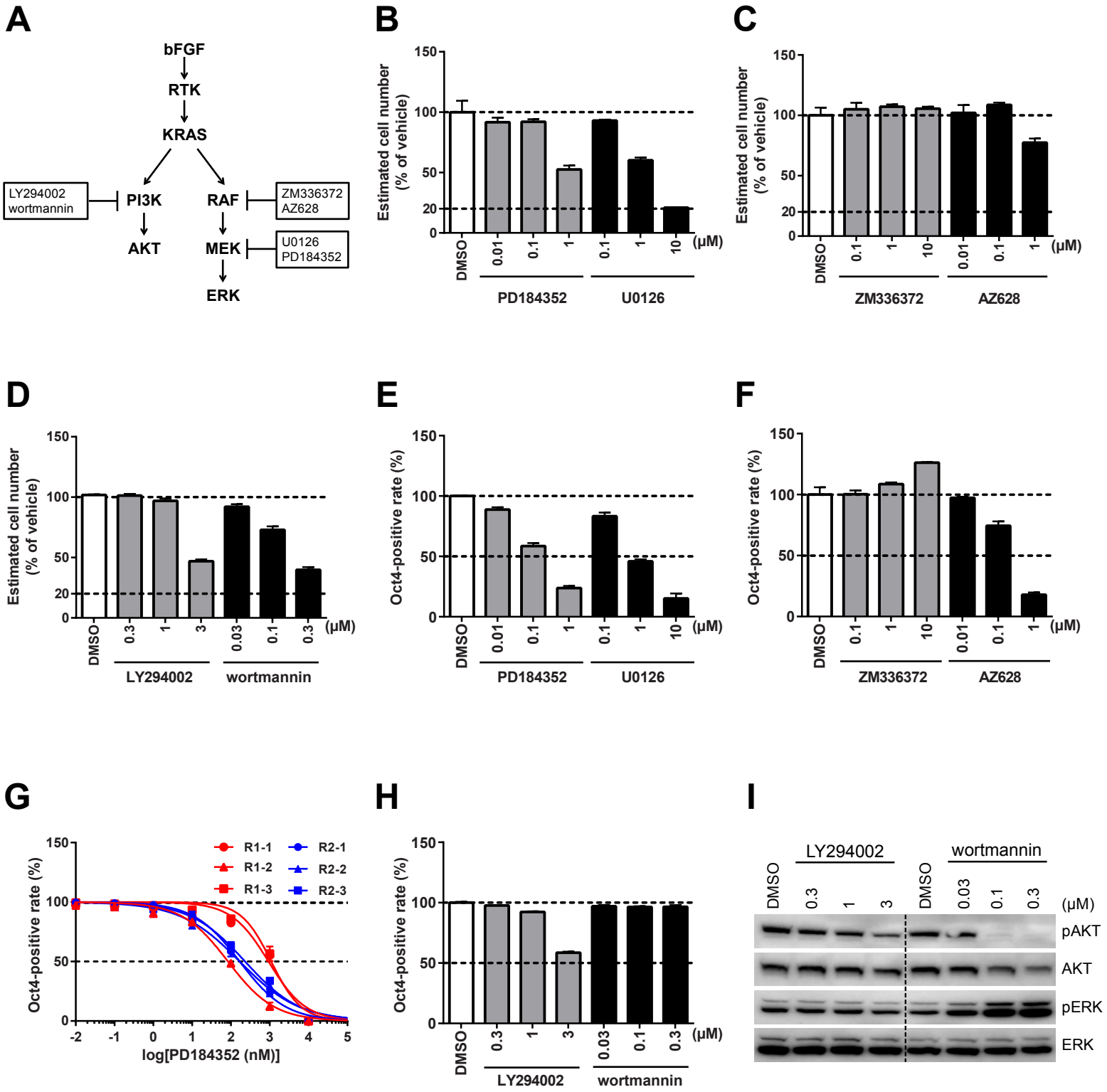
A
bFGF
RTK
KRAS
LY294002
wortmannin
PI3K
RAF
ZM336372
AZ628
AKT
MEK
U0126
PD184352
ERK
B
Estimated cell number (% of vehicle)
DMSO
PD184352
U0126
(μM)
C
Estimated cell number (% of vehicle)
DMSO
ZM336372
AZ628
(μM)
D
Estimated cell number (% of vehicle)
DMSO
LY294002
wortmannin
(μM)
E
Oct4-positive rate (%)
DMSO
PD184352
U0126
(μM)
F
Oct4-positive rate (%)
DMSO
ZM336372
AZ628
(μM)
G
Oct4-positive rate (%)
R1-1
R1-2
R1-3
R2-1
R2-2
R2-3
log[PD184352 (nM)]
H
Oct4-positive rate (%)
DMSO
LY294002
wortmannin
(μM)
I
LY294002
wortmannin
DMSO
(μM)
pAKT
AKT
pERK
ERK

Figure S5. Pharmacological analysis on the involvement of the RAF–MEK–ERK and PI3K–AKT pathways in enforced retention of self-renewal of RALD patient-derived iPSCs (Related to Figure 6)

(A) bFGF-pathway and kinase inhibitors used in this study. (B–D) Effects of MEK inhibitors (PD184352 and U0126) (B), RAF inhibitors (ZM336372 and AZ628) (C), and PI3K inhibitors (LY294002 and wortmannin) (D) on cell numbers of G13C/WT iPSCs (clone R1-2), estimated by counting the number of Hoechst-stained nuclei relative to DMSO-treated cells (n = 3 independent experiments; mean ± S.E.M.). (E and F) Effects of MEK inhibitors (PD184352 and U0126) (E) and RAF inhibitors (ZM336372 and AZ628) (F) on OCT4-positive areas in G13C/WT iPSCs (clone R2-1) cultured without bFGF for 5 days (n = 3 independent experiments; mean ± S.E.M.). (G) Effects of PD184352 on OCT4-positive areas in all clones (n = 3 independent experiments; mean ± S.E.M.). (H) Effects of PI3K inhibitors (LY294002 and wortmannin) on OCT4-positive areas in G13C/WT iPSCs (clone R1-2) cultured without bFGF for 5 days (n = 3 independent experiments; mean ± S.E.M.). (I) Western blot analysis of G13C/WT iPSCs (clone R1-2) cultured without bFGF for 2 days. ERK and AKT were analyzed for their phosphorylation.

Table S1. Clinical information of two RALD patients (Related to Figure 1)

	Case no. 1	Case no. 2*
Sex	Male	Male
Mutation (*KRAS*)	G13C (GGC > TGC)	G13C (GGC > TGC)
Lymphoadenopathy	Positive	Negative
Hepatosplenomegaly	Positive	Negative
GM-CSF hypersensitivity	Not assessed	Negative
Autoantibody	Positive	Negative
White blood cells (/L)	4.6×10^9	8.4×10^9
Monocytes (/μL)	690	336
Blasts (/μL)	0	0
Platelets (/L)	48×10^9	22×10^9
Hemoglobin (g/dL)	9.9	8.5
IgG (mg/dL)	2749	1018
Medication	prednisolone, mycophenolate mofetil	prednisolone, adalimumab, colchicine, salazosulfapyridine

*(Moritake et al., 2016)

Table S2. Information of iPSCs clones derived from two RALD patients (Related to Figure 1)

Patient	Karyotype	*KRAS* genotype	Original clone name	Clone name in this paper	Passage number at introduction into Eisai Co., Ltd.
Case no. 1	46XY	WT/WT	TKSRC1_#1	C1-1	8
		G13C/WT	TKSR1_#30	R1-1	9
			TKSR1_#37	R1-2	8
			TKSR1_#40	R1-3	8
Case no. 2	46XY	WT/WT	TKSRC2_#1	C2-1	12
			TKSRC2_#8	C2-2	12
			TKSRC2_#11	C2-3	11
		G13C/WT	TKSR2_#10	R2-1	12
			TKSR2_#21	R2-2	12
			TKSR2_#26	R2-3	10

Table S4. Summary of two-way ANOVAs evaluating data of Figures 4C and S3D (Related to Figures 4 and S3)

Data	Effects	SS	DF	MS	F	P
Case no. 2 clones related to Figure 4C	bFGF treatment	7353	1	7353	740.1	<0.001
	KRAS genotype	5331	1	5331	536.6	<0.001
	bFGF treatment × *KRAS* genotype	5064	1	5064	509.6	<0.001
	Residual	79.49	8	9.936		
Genome-edited clones related to Figure S3D	bFGF treatment	80060	1	80060	11832	<0.001
	KRAS genotype	35720	5	7144	1056	<0.001
	bFGF treatment × *KRAS* genotype	37596	5	7519	1111	<0.001
	Residual	568.4	84	6.767		

SS, sum of squares; DF, degrees of freedom; MS, mean square; F, F statistic; P, P value.

Table S5. IC_{20}, IC_{50}, and IC_{80} values of PD184352 (Related to Figure 6)

Clone	IC_{20} (nM)	IC_{50} (nM)	IC_{80} (nM)
R1-1	336.7 ± 110.7	1156.4 ± 150.3	4268.3 ± 311.8
R1-2	12.5 ± 0.7	74.9 ± 5.7	452.1 ± 58.281
R1-3	657.1 ± 170.6	1399.3 ± 154.4	3197 ± 288.04
R2-1	30.3 ± 4.7	284.4 ± 111.7	2942.7 ± 1777.9
R2-2	12.3 ± 3.2	125.2 ± 27.2	1312.4 ± 317.05
R2-3	19.5 ± 2.5	336.3 ± 148.6	8498 ± 6718.4

Data are expressed as mean ± S.E.M. from three independent experiments.

Table S6. Antibody list used in this study

Antigen	Host/Isotype	Supplier	Cat No	Dilution ratio	Application
OCT4	Mouse/IgG2b	Santa Cruz Biotechnology	sc-5279	1:100	ICC 1st Ab
NANOG	Rabbit/IgG	PeproTech	500-P236	1:200	
SSEA4	Mouse/IgG3	Millipore	MAB4304	1:500	
TRA-1-60	Mouse/IgM	Millipore	MAB4360	1:500	
MAP2	Rabbit/IgG	Millipore	AB5622	1:500	
βIII-Tubulin	Mouse/IgG2b	Sigma	T8660	1:1000	
Mouse IgG	Donkey/IgG (AF488)	Thermo Fisher Scientific	A21202	1:500	ICC 2nd Ab
Mouse IgG	Donkey/IgG (AF555)	Thermo Fisher Scientific	A31570	1:500	
Rabbit IgG	Donkey/IgG (AF555)	Thermo Fisher Scientific	A31572	1:500	
Mouse IgM	Goat/IgG (AF488)	Thermo Fisher Scientific	A21042	1:500	
ERK	Rabbit/IgG	Cell Signaling Technology	4695	1:2000	WB 1st Ab
phospho-ERK	Rabbit/IgG	Cell Signaling Technology	9101	1:1000	
Akt	Rabbit/IgG	Cell Signaling Technology	9272	1:2000	
phospho-Akt	Rabbit/IgG	Cell Signaling Technology	4060	1:2000	
KRAS	Rabbit/IgG	Santa Cruz Biotechnology	sc-521	1:100	
β-Tubulin	Mouse/IgM	Santa Cruz Biotechnology	sc-53140	1:3000	
Mouse IgG/IgM	Sheep/IgG (HRP)	GE Healthcare	NA931-1ML	1:2500	WB 2nd Ab
Rabbit IgG	Donkey/IgG (HRP)	GE Healthcare	NA934-1ML	1:2500	

Ab, Antibody; ICC, Immunocytochemistry; WB, Western blotting; AF, Alexa Fluor; HRP, Horseradish peroxidase.

Table S7. Sequence list of primers and a donor oligo used in this study

Direct sequencing		Sequence (5’ > 3’)
KRAS	Fwd	TTCTTAAGCGTCGATGGAGGAG
	Rev	AGAGTGAACATCATGGACCCTG
Off-target 1	Fwd	TGGAATGAGCTTTGACTGCCT
	Rev	AGGACCATAGGCACATCTTCAG
Off-targets 2 and 3	Fwd	CTGGGAGCTGAAGGACATGG
	Rev	GGGTCATAATGTTTGCCCCG
Off-target 4	Fwd	TGAAGATGCACTGGGCTCTG
	Rev	GGCTGCTTCTTCCTAGCCAT
Off-target 5	Fwd	AGCCACTGACCCTTTATGGC
	Rev	TCTCTTCTTCCTGCCCCAGA
Genome editing		Sequence (5’ > 3’)
sgRNA	Fwd	ACCGTTGGAGCTGGTTGCGT
	Rev	AAACACGCAACCAGCTCCAA
Donor (ssODN)		A*****C*****A*****AAATGATTCTGAATTAGCTGTATCGTCAAGGCACTCTTGCCTACGCCGC CGGCTCCAACTACCACAAGTTTATATTCAGTCATTTTCAGCAGGC*****C*****T*****T

sgRNA, single guide RNA; ssODN, single-stranded oligodeoxynucleotide; Fwd, Forward; Rev, reverse; *****, phosphorothioate.

Supplemental Experimental Procedures

Case description of RALD patients

A boy (case no. 1) has exhibited thrombocytopenia since 13 years old. Lymphoadenopathy and splenomegaly have been noted since 18 years old. Pancytopenia also appeared at age of 19. Blood test exhibited various autoimmunity signs. Molecular testing was performed at 19 years old, and revealed the presence of the *KRAS* G13C mutation. Immunosuppressive therapy including prednisolone and mycophenolate mofetil has been performed since then. As of 2017, he is 25 years old, and exhibits hepatomegaly and ulcer at colon. Regarding the patient of case no.2, a detail report was published previously (Moritake et al., 2016). Clinical information of the two RALD patients is summarized in Table S1.

Genome editing

Genome editing was performed as previously described (Uehara et al., 2017). Briefly, 1×10^6 cells were nucleofected with 2 μg of pEF1-Cas9-2A-AzamiGreen, 2 μg of pU6-gRNA, and 1 μg of single-stranded oligodeoxynucleotides using a Human Stem Cell Nucleofector Kit 1 (Lonza) and seeded on a vitronectin-coated 6-well plate in StemFit containing 10 μM Y-27632 (Wako). The oligonucleotides used in genome editing are listed in Table S7. Cas9 transfectants were collected by a FACS SH800 (Sony) on day 2 post-nucleofection and seeded on 10 cm culture dishes for single cell cloning. Clones were manually picked after 7-day culture and transferred to wells of 96-well plates. For genotyping, genome of each clone was extracted, followed by restriction enzyme fragment length polymorphism (RFLP) assays. Briefly, cells were incubated in TE buffer containing 0.1% SDS (w/v) and 1 μg/ml protease K at 55°C overnight, followed by 95°C for 10 min. The target region was amplified by a standard nested PCR protocol using NEBNext (NEB) and PCR fragments were digested by *Nae*I (NEB) for RFLP assays to screen edited clones. Sequences of hit clones in RFLP assays were confirmed by Sanger sequencing using ABI3130XL (Applied Biosystems).

Direct sequencing

Genomic DNA was purified with NucleoSpin Tissue XS (Takara) according to the manufacturer's protocol. PCR was performed by a standard technique with NEBNext DNA Polymerase (NEB). All the PCR primers are indicated in Table S7. PCR products were then cleaned up by an ExoSAP-IT (Affimetrix), and sequenced with an ABI3130XL (Applied Biosystems).

Quantitative real time-PCR

Total RNA was extracted and purified by using an RNeasy kit (Qiagen) following manufacturer's instructions.

Reverse transcription was performed with 100 ng of total RNA using SuperScript VILO Master Mix (Thermo Fisher Scientific). For qRT-PCR, each reaction mixture of total 12 μL contained 0.6 μL of TaqMan probe, 6 μL of EagleTaq Universal Master Mix (Roche), and cDNA. All qRT-PCR reactions were performed using ABI 7900 (Applied Biosystems). Reactions were performed at 95°C for 10 min followed by 45 cycles of 95°C for 15 s and 60°C for 1 min. Fold changes were calculated relative to 18S ribosomal RNA. The following TaqMan probes were used: POU5F1 (Hs04260367_gH), NANOG (Hs04399610_g1), FOXA2 (Hs00232764_m1), SOX17 (Hs00751752_s1), EOMES (Hs00172872_m1), T (Hs00610080_m1), PAX6 (Hs00240871_m1), ASCL1 (Hs04187546_g1), and 18S ribosomal RNA (Hs99999901_s1). All TaqMan probes were purchased from Applied Biosystems.

Whole exome sequencing (WES)

WES analysis was performed based on standard protocol. Briefly, genomic DNA was fragmented, and exonic sequences were enriched using SureSelect Human All Exon 38Mb kit (Agilent). The captured fragments were purified and sequenced on a Hiseq2000 platform (Illumina). Bioinformatic analysis was performed using an in-house algorithm.

RNA sequencing (RNA-seq)

RNA-seq was performed to compare gene expression profiles between WT/WT and G13C/WT iPSCs before and after *in vitro* differentiation for 16 days. Total RNA was extracted and purified by using an RNeasy kit (Qiagen) following manufacturer's instructions. The concentration of purified RNA was measured with a NanoDrop 2000 spectrophotometer (Thermo Fisher Scientific), and its quality was assessed with a 2100 Bioanalyzer (Agilent). The total RNA (1μg) was converted into cDNA library for Illumina multiplex sequencing by using SureSelect Strand-Specific RNA Library Prep kit (Agilent) in accordance with the manufacturer's protocol. The fragment length and quality of cDNA library was assessed with a 2100 Bioanalyzer, and the concentration was determined by using KAPA library quantification Kit (NIPPON Genetics). RNA sequencing was performed using NextSeq 500 (Illumina). The raw reads were trimmed for raw quality reads by Trimmomatic (Bolger et al., 2014). The reads were mapped to human transcriptome annotations and reference genome sequence (Ensemble 88, GRCh38) using STAR (Dobin et al., 2013). RSEM was used for estimating gene-level expression reported as TPM (transcripts per million) with strand-specific option (Li and Dewey, 2011).

Microarray analysis

Microarray analysis was performed as previously described (Uehara et al., 2017). The data were analyzed with

GeneSpring 13.1 software (Agilent), and the raw data were normalized by using a quantile method.

Western blotting

Cells were lysed in sample buffer containing PhosSTOP (Roche), protease inhibitor cocktail (Roche), and 1 mM dithiothreitol (DTT), followed by protein quantitation using 660 nm Protein Assay Reagent (Thermo Fisher Scientific). Equal amounts of samples were resolved by sodium dodecyl sulfate-polyacrylamide gel electrophoresis (SDS-PAGE) and western blotting according to standard protocols. Detailed conditions of antibodies are given in Table S6. The signal was visualized by chemiluminescence using LuminataForte HRP substrate (Millipore) with a LAS4000 imager (Fujifilm). The densitometry of each band was quantified by an ImageQuant TL (GE Healthcare).

Expression and purification of recombinant RAF1-RBD

GST-RAF1-RAS-binding domain (RBD) (1–149 amino acids) was cloned into pGEX-6P-1 at the *Bam*HI/*Sal*I site by a standard protocol. For expression of the recombinant protein, the plasmid was transformed into BL21 and cultured in LB medium containing ampicillin (Wako) at 37°C, followed by 0.5 mM isopropyl β-D-1-thiogalactopyranoside (Wako) induction at optical density of 0.6 and further incubation at 15°C for overnight. Bacterial cells were lysed by BugBuster Protein Extraction Reagent (EMD Millipore) and GST-RAF1-RBD was purified by Glutathione Sepharose 4B (GE Healthcare) according to the manufacturer's protocol. Eluted samples were dialyzed in binding buffer (50 mM Tris-HCl, 150 mM NaCl, 2 mM $MgCl_2$, 1% (v/v) NP-40, 10% (v/v) glycerol, and 1 mM DTT; pH 7.5) and stored at –80°C.

RAF1-RBD pull-down assays

Cells were lysed in binding buffer (50 mM Tris-HCl, 150 mM NaCl, 2 mM $MgCl_2$, 1% (v/v) NP-40, 10% (v/v) glycerol, and 1 mM DTT; pH 7.5) containing the PhosSTOP and protease inhibitor cocktail. Cell lysates were centrifuged and supernatants were incubated with 25 μg of purified glutathione *S*-transferase (GST)-RAF1-RAS-binding domain (RBD) and glutathione sepharose beads (GE Healthcare) at 4°C for 3 h. The beads were washed three times with the binding buffer, and proteins were eluted by 2× sample buffer (120 mM Tris-HCl, 4% (w/v) SDS, 20% (v/v) glycerol, and 0.02% bromophenol blue; pH 6.8), followed by western blotting to detect RAF1-bound KRAS. A part of cell lysates was used for detecting input KRAS and β-Tubulin. Western blotting was performed as described above.

Statistical analysis

All data are expressed as means ± standard errors of means (S.E.M.). GraphPad Prism 6.0 (GraphPad Software)

was used for preparation of concentration-response curves, calculation of IC_{20}, IC_{50}, and IC_{80} values, and statistical comparison. Data of bFGF-depletion assays were examined effects of KRAS genotypes and bFGF conditions (its presence and absence) by two-way factorial analysis of variance (ANOVA), followed by Bonferroni's multiple comparison test as a post hoc test. For western blotting and GST-RAF1 pull-down assays, differences between the two genotypes (WT/WT and G13C/WT) were examined by two-tailed unpaired Student's *t*-test or Mann-Whitney's test, and those among the three genotypes (Δ^{ed}/WT, WT^{ed}/WT, and G13C/WT) were examined by one-way factorial ANOVA, followed by Bonferroni's multiple comparison test as a post hoc test. Data of the MEK inhibitor treatment in an *in vitro* differentiation were analyzed by one-way factorial ANOVA, followed by Dunnett's test. A probability value (p) < 0.05 was considered statistically significant.

Supplemental References

Bolger, A.M., Lohse, M., and Usadel, B. (2014). Trimmomatic: a flexible trimmer for Illumina sequence data. Bioinformatics (Oxford, England) *30*, 2114-2120.

Dobin, A., Davis, C.A., Schlesinger, F., Drenkow, J., Zaleski, C., Jha, S., Batut, P., Chaisson, M., and Gingeras, T.R. (2013). STAR: ultrafast universal RNA-seq aligner. Bioinformatics (Oxford, England) *29*, 15-21.

Li, B., and Dewey, C.N. (2011). RSEM: accurate transcript quantification from RNA-Seq data with or without a reference genome. BMC bioinformatics *12*, 323.

Moritake, H., Takagi, M., Kinoshita, M., Ohara, O., Yamamoto, S., Moriguchi, S., and Nunoi, H. (2016). Autoimmunity Including Intestinal Behcet Disease Bearing the KRAS Mutation in Lymphocytes: A Case Report. Pediatrics *137*, e20152891.

Uehara, T., Minoshima, Y., Sagane, K., Sugi, N.H., Mitsuhashi, K.O., Yamamoto, N., Kamiyama, H., Takahashi, K., Kotake, Y., Uesugi, M., *et al.* (2017). Selective degradation of splicing factor CAPERalpha by anticancer sulfonamides. Nature chemical biology *13*, 675-680.